J Nanostruct 11(4): 802-813, Autumn 2021

RESEARCH PAPER

Thin Films Microstructure, Thickness and Electrical Resistivity of Electrodeposited $Ni_{1-x}Fe_x$/ITO/Glass, Abnormal Alloy under OverallT <110> onto <211> Tilt

Fatima Nemla [1,2]*, *Djellal Cherrad* [1,3]

[1] *Laboratoire de développement de nouveaux matériaux et de leurs caractérisations, Université de Sétif, Algérie.*

[2] *Ecole Normale Supérieure de Sétif-ENSS, Algérie*

[3] *Département de physique, Faculté des Sciences, Université de Sétif 1 Algérie.*

ARTICLE INFO

Article History:
Received 28 June 2021
Accepted 04 September 2021
Published 01 October 2021

Keywords:
Electrical measurements
$Ni_{1-x}Fe_x$/ITO/Glass
SEM-TFE-EDS
Texture tilt, XRD technique
Thin films
Van Der Paw electrical measurements

ABSTRACT

In this work, the electrodeposition of $Ni_{1-x}Fe_x$/ITO/Glass, thin films in sulfate bath was carrying out in the present work. The XRD technique, Scanning Electron microscopy SEM and EDS, Van Der Paw electrical measurements, have been used as principal work techniques to investigate the structural, compositional and electrical properties of $Ni_{1-x}Fe_x$ obtained at different electrodeposition times. Thickness, roughness and surface quality were investigated by the medium of contact stylus profilometry measurement technique. The grain size D values were found to change in the range of 48 until 106 nm. It was shown that primary texture <110> tilt onto <211> at the 1080 s electrodeposition time. This may take part of abnormal behavior in our films. Electrical resistivity ρ, average grain size D, thickness t and roughness are majorly affected by overall texture tilt and present correlations between each other's. $Ni_{1-x}Fe_x$ films micrographs have been served for confirmation and achievement of the present work.

How to cite this article
Nemla F., Cherrad D. Thin Films Microstructure, Thickness and Electrical Resistivity of Electrodeposited $Ni_{1-x}Fe_x$/ITO/Glass, Abnormal Alloy under OverallT <110> onto <211> Tilt. J Nanostruct, 2021; 11(4): 802-813. DOI: 10.22052/JNS.2021.04.017

INTRODUCTION

The alloy preparation by physical or metallurgical methods presents a large advantage of a fine composition and smooth control but, sincerely, with a high production cost. Therefore, due to the low fabrication costs, great purity of the deposits, and large choice of the piece shapes, the Electrodeposition make often the best technique to prepare many alloys and systems. In last decades, the number of papers on the electrodeposition of alloys has increased indicating a promising use of this film preparation method. Moreover, the deposition of ferromagnetic coating is thus one of the most important development of electroplating because of ever-increasing use of thin films in microelectronic, computers and data handling technology and some other fields.

Ni-Fe alloys have been intensively investigated during the last decade for their unique physical properties such as mechanical [1] and magnetic [2] properties, which was known to form soft magnetic coating. The composition of soft magnetic alloys and their properties have been reported in the earlier works of Morika and Tanhaschi [3], Wolf [4, 5], Wolf and Katz [6], Bozart [7], Tsu and Sallo [8], Smith *et al*. [9] and Avdeeva [10].

Such NiFe alloys are electrodeposited from Chloride, Sulphate, mixed or sulphamate baths were reported to be among the most interest

* *Corresponding Author Email: fati_nemla@yahoo.fr*
f.nemla@ens-setif.dz

nowadays because they yield deposits with the lowest internal stress [11]. It is well known that Ni displays a corrosion resistance greater than iron in most environments and that NiFe alloys show intermediary behavior.

New applications of Invar ($Fe_{64}Ni_{36}$) have been proposed, such as structural reinforcement in monument restorations and glass roofs repairs in historical and cultural buildings. [12]. Because of Ni-Fe alloys similarity to the Invar, many attentions have been devoted to them. Report that for this atomic composition, a change of the crystal structure (from bcc for the Fe-rich alloys to fcc for the systems with higher Ni concentration) appears [13, 14, 15]. The deposition of Ni-Fe alloy is called abnormal [16], this is because of the famous raison given the fact that the less noble element (iron) is deposited preferentially before the noblest (nickel) element; as well the amount of iron in the deposit will not be connected to its portion in the electrolyte. From a sulphate bath, Dahms et *al*. [17] have been studied electrodeposited NiFe on a rotating electrode. They have found that increasing in deposited iron amount is directly related to a decrease in the velocity of nickel deposition. Krause et *al*. [18] have showen that abnormal co-electrodeposition plating NiFe alloy is due, essentially, to iron hydroxide $Fe(OH)_2$ precipitation at the surface of the electrode.

In view of the previously cited papers, we are aware that NiFe alloy is deeply investigated since the few last decades. However, to the best of our knowledge, there are few experimental works exploring the dependence in electrodeposition time of microstructure, thickness and electrical resistivity of $Ni_{1-x}Fe_x$/ITO/Glass, abnormal alloy. On the other side, We had ambition to employ unusual potential range between -1.45 V and -1.48 V, since the majority of old published reports using the same method as ours, usually do not exceed -1.35 V during their electrodeposition. This can reveal hidden properties of $Ni_{1-x}Fe_x$ if samples are successfully elaborated. Moreover, we aim to contribute towards the understanding of existing correlation between different properties (structural parameters, electrical resistivity and morphological properties).

MATERIALS AND METHODS

$Ni_{1-x}Fe_x$ thin films were prepared by electrodeposition onto commercial polycrystalline indium tin oxide (ITO) covered glass substrate which possess about 10 Ω/cm; (measured in area of 1×2 cm^2 exposed to the electrolyte), as square resistance. All the depositions were made in a three electrodes cell containing Ni as a counter electrode, silver-silver chloride (Ag/AgCl) as reference and ITO coated glass as a working electrode. We have chosen the ITO substrate as cathode because of its high transparence and its properties as inert material. Before electrodeposition, ITO glass was first cleaned with acetone for 30 min and then alcohol for 30 min, finally rinsed in distilled water. A potensiostat/ galvanostat system"parstat 2253" was utilized for preparing our alloy samples. In Fig. 1. We illustrate a real photo of the electrodeposition equipment that we have used with two others photos insets for the preparation process of $Ni_{1-x}Fe_x$ thin films. However, visualization of *V=f(I)* allure is obtained via PowerSuite software that is implemented in the parstat 2253 . The electrolyte [0.1] (see In Table 1) was freshly prepared. The used Boric acid (adjusted to 2.7 using diluted H_2SO_4) was added to the bath in order to control the pH of the solution also to improve the quality of the deposit. In addition, Saccharin has been used as an organic additive to reduce the internal stress of deposits and to refine the grain structure [19]. $Ni_{1-x}Fe_x$ thin films were deposited at a cathode potential of -1.45 (vs. Ag/AgCl). After carful test, we have deduced that the above study potential was the best ones to reach higher efficiency electrochemical deposition. For then, all time depositions were obtained at this potential. Electrodeposition was performed at room temperature, without stirring. Unlike several previous report we have successfully electrodeposited $Ni_{1-x}Fe_x$ thin films onto semiconductor ITO substrate.

X-ray diffraction (XRD) analysis, using a Philips X'Pert diffractometer with CuKα (λ=1.54 Å) radiation is employed for determining structural properties. Veeco Dektak 150 surface profilometer using contact stylus profilometry measurement technique was employed to investigate film thicknesses, roughness and surface quality. Scanning Electron Microscope, high power optics Thermal Field Emission (SEM –TFE) JSM 7001F/ JSM 7001FA deliver surface images and film composition. Square (sheet) resistance and the electrical resistivity were inferred from a Van Der Paw four-point cell measurements set-up (using the ECOPIA HMS-3000 system from Bridge Technology).

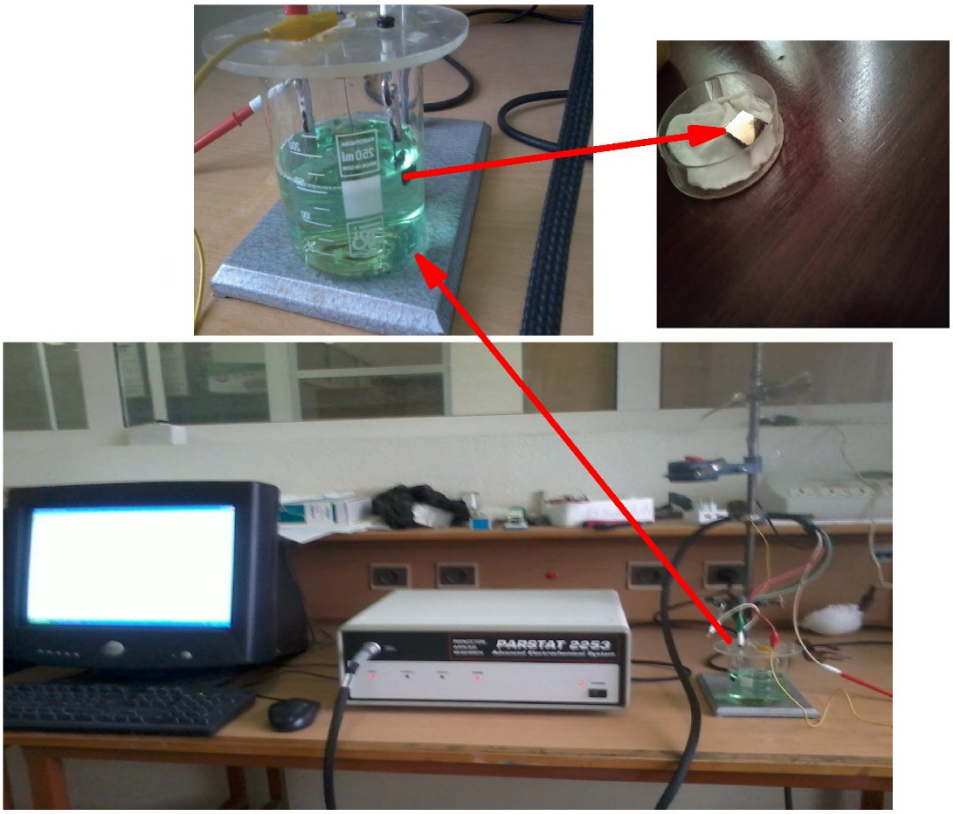

Fig. 1. Photo of used electrodeposition equipment for the preparation process of $Ni_{1-x}Fe_x$ thin films. Photos insets represent the sulphate work bath and sample post-electrodeposition

Table 1. Sulfate bath electrolyte composition and utilized parameters for electrodepositing $Ni_{1-x}Fe_x$ films onto ITO/Glass.

Bath composition	0.036 M $NiSO_4{\cdot}6H_2O$
	0.064 M $(NH_4)_2$ Fe $(SO_4).6H_2O$
	12.5g NaCl
	0.5 g H_3BO_3
	0.2$C_{12}H_{25}NaO_4S$
	0.5 Saccharin
	pH 2.7
Operating parameters	Temperature (°C) 20-25
Cathode	ITO
Anode	Ni

RESULTS AND DISCUSSION

Structural analysis and electrodeposits composition

Structural analysis of electrodeposited $Ni_{1-x}Fe_x$/ITO/glass, films at room temperature was characterized by XRD technique. In first stage, for a fixed 600 s electrodeposition duration, four electrodeposits were prepared at -1.45, -1.46, -1.47 and -1.48 V electrochemical potentials. In second stage, we have chosen to fix electrochemical potentials at -1.45 V while changing electrodeposition duration each time as 600, 720, 840, 960, 1080, 1200 s to obtain six other $Ni_{1-x}Fe_x$/ITO/glass, films. Fig. 2.a shows the XRD patterns of our first stage study of $Ni_{1-x}Fe_x$ films obtained for 600 s and deposited with -1.45, -1.46, -1.47 and -1.48 V, respectively. Indeed, the peaks marked with star (*) are assigned to the ITO coated conducting glass substrates. But, the four other peaks at 2θ values of 41.65°, 44.28°, 47.6°, and 51.50° might be attributed, respectively, to the textures <110> <200> <220> and <211> of

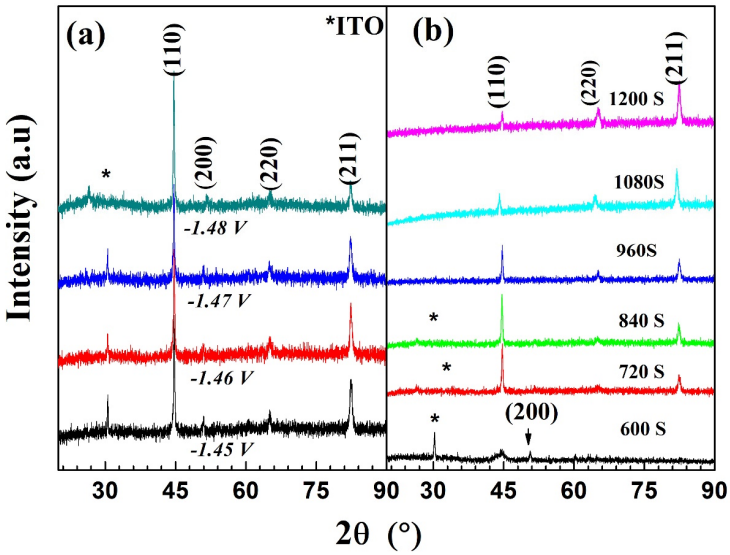

Fig. 2. XRD patterns of $Ni_{1-x}Fe_x$/ITO/Glass studied films deposited at room temperature (a) at different potentials, (b) at different electrodeposition time. (*) For ITO diffraction peaks.

Table 2. Lattice parameters a (Å), Fe content (wt. %), of $Ni_{1-x}Fe_x$ films at different electrodeposition time onto ITO/Glass electrode.

Time, t(s)	*a(Å)*	*Fe content (wt. %)*
600	2.8598	92.159
720	2.8589	84.696
840	2.8647	85.568
960	2.8607	86.579
1080	2.8692	81.611
1200	2.8533	85.360

the body centered crystal "bcc" polycrystalline adopted structure. Overall texture is dominated (110) reflexion with small co-existence of Invar alloy presented by (200) reflexion revealed in film elaborated particularly at 600 s (see Fig.2.b). This result is expected for our films with high Fe content. Our result about the overall texture is entirely consistent with that of Chang Su-wei et *al* [20]. The authors have suggested that the (110) orientation is preferred and dominant when the overall texture crystallizes in bcc structure while the (111) orientation is preferred and dominant when it is fcc crystallization [20-21].

As mentioned in Table 2, films composition take change in the range of 81–92 (wt.% Fe). According to I.Tabakovic et *al* [21] This compositional range show that dominant structures tilt into bcc $Ni_{1-x}Fe_x$ alloys.

Indeed, changing time electrodeposition between 600s and 1200 s have not affected considerably $Ni_{1-x}Fe_x$ films composition comparing to other effects cited in literature such as the precursor PH, annealing, mechanical alloying…etc. [22-23]. In Fig. 3. We have chosen EDS spectrum for film that was obtained at 600s as demonstrator sample which is characterized by the highest content of Fe.

Generally, crystallization tilt into the structure of dominating chemical element is such NiFe alloys. In addition, It was reported [21] that X-ray investigation of electrodeposited $Ni_{1-x}Fe_x$ films at room temperature reveal the existence of fcc or γ phase in the range of 10-58 wt.% Fe, mixed fcc/bcc phase in the range of 59-63 wt.% Fe, and purely bcc or α phase in the range of 64-90 wt.% Fe.

A suddenly changing in crystalline texture (see Fig.2) at 1080 second from <110> into <211> is another fact which can be considered as a pointed result and might be connected with a new criterion of abnormal behaviour in our $Ni_{1-x}Fe_x$ studied alloy. To the best of our knowledge, there is no report on $Ni_{1-x}Fe_x$ alloy have mentioning this texture change before. That one paper of B. Ghebouli et *al* [24] which have reported texture tilt from <110> into

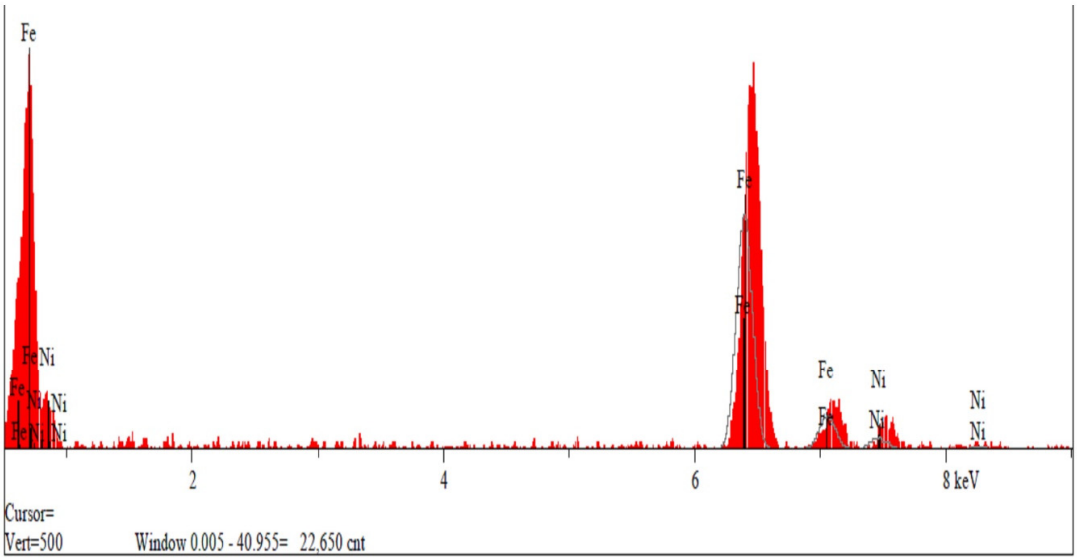

Elt.	Line	Intensity (c/s)	Conc	Units	Error 2-sig	MDL 3-sig
Fe	Ka	255.27	92.159	wt.%	4.574	1.927
Ni	Ka	12.80	7.841	wt.%	2.605	3.058
			100.000	wt.%		Total

Fig. 3. EDS spectrum of $Ni_{0.08}Fe_{0.92}$ film electrodeposited on ITO coated conducting glass substrate.

<211> in pure evaporated Fe/glass layers. It is to be noted here that lattice parameter of pure iron in ICPDS file is 0.28664 nm close to our obtained ones since the content of Fe was greater than 80%. Xiaobai Chena et *al* [25] have discussed structural phase transformation and have found for sputter deposited NiFe thick films obtained with different composition that lattice parameter is 0.35866 nm for annealed $Ni_{33}Fe_{67}$ film at 753K and was found to be 0.28442 nm for the as-deposited $Ni_{21}Fe_{79}$ film.

Addionaly, we can note, here, that in spite of changing potential deposition, the $Ni_{1-x}Fe_x$ alloy textures remained unchanged and <200> texture did not yet disappear. Generally, the increase in lattice parameters in $Ni_{1-x}Fe_x$ alloy has been found leading to the solid solution formation or the amorphous phase formation [26]. With increasing time deposition, it can be seen that the lattice parameter of $Ni_{1-x}Fe_x$ samples deviates slightly by less than 1% (about 0.55 %) during all deposition times (see Table 1). Literally, lattice parameter have not detected the disordering induced by electrodeposition whether when we enhance time or potential during electrodeposition. R. Hamzaoui et *al* [27] have suggested that the value of the lattice parameter take a small increases from a=0.286599±0.00005 to 0.287049±0.00005 nm which was resulting from 96 h of milling for $Fe_{0.9}Ni_{0.1}$ alloy and from a= 0.286589±0.00005 to 0.287069±0.00005 nm for $Fe_{0.8}Ni_{0.2}$ alloy.

Surface quality and roughness

Using contact stylus profilometry measurement technique allow review of surface quality and curvatures as well as thickness measurement. As illustrated in Fig. 4. Bi-dimensional surface scan show curvatures in deep and high for all samples. More curvatures are revealed within potentials changes especially at -1.47V (Fig.4.a). One can remark that there is no considerable a deep grooves or defects that can reflect structural or electrical properties worsening (Fig.4.a and b). All films have a mirror behaviour of good metallic character, no peels or bubbles on the top of all films surface. Several tests that we have carrying out before adoption of the present samples allow

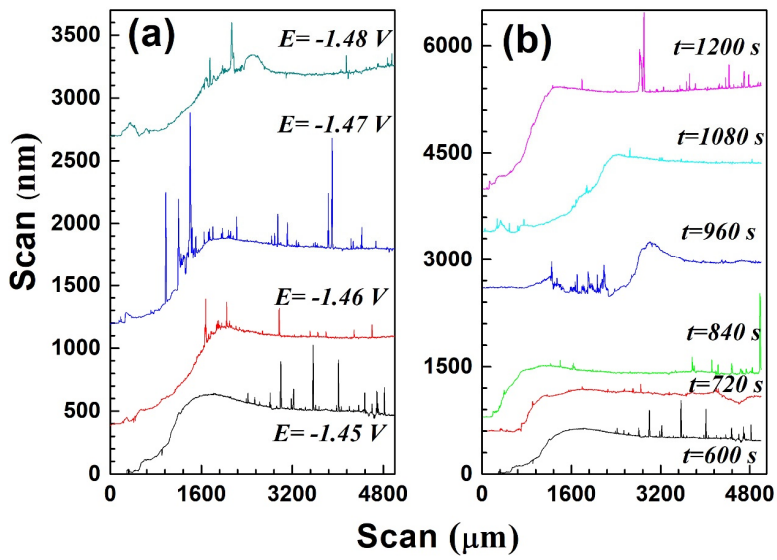

Fig. 4. Surface quality scanning roughness and waviness profiles for $Ni_{1-x}Fe_x$ samples: (a) different electrodeposition potential; and (b) different times.

Table 3. Grain Size (D), Thickness (e), Sheet resistance (Rsq) and roughness obtained for different electrodeposition time of $Ni_{1-x}Fe_x$ onto ITO/Glass electrode.

Time, t(s)	*Grain Size, D(nm)*	*Thickness ,e(nm)*	*Roughness (nm)*	*Sheet resistance, R_{sq} (Ω/cm)*
600	97.5	520	103	0.04079
720	55.77	530	75	0.04843
840	48.68	625	98	0.12607
960	48.73	720	138	0.13069
1080	99.32	960	113	0.00356
1200	106.02	1400	98	$9.69494\ 10^{-4}$

us to observe extreme conditions of the present electrodeposition. Beyond -1.47V and/or 1200 second electrodeposition duration, surface appear peeled and bubbled that's why we have limited our conditions. Indeed, film surface at 1080 s tilted overall texture appear the smoothest with the less curvatures (see Fig.4.b), thus may relate to best structural stability. Surface roughness values obtained for various time electrodeposition are mentioned in Table. 3. Values changes between 75 nm and 138 nm that seems, for first view, to have an aleatory evolution versus electrodeposition time.

Grain size evolution under dominant texture tilt

The average grains size *D* in our films take a change in the general range of 48-106 nm (see Table 3). The increase of grain size in NiFe alloy can be assigned to coalescence and agglomeration since smaller grains. S. Sam et *al* [28] have result to the average grain size of about 16 nm for $Ni_{81}Fe_{19}$ compositional film and about 23 nm for $Ni_{83}Fe_{17}$ film. Whereas, C. Cheung et *al* [29] have suggested that electrodeposited $Ni_{1-x}Fe_x$ Permalloy grain size were calculated to be 10 nm. In the case of those authors which they have suggest a bigger size of grains, we found T.E. Buchheit et *al* [30]. These last authors have reported twice that electrodeposited $Ni_{1-x}Fe_x$ Permalloy $Ni_{80}Fe_{20}$ grain size was found to be less than 100 nm.

Two distinct case depending on dominant over all texture are clearly revealed. In first stage, when dominant texture was <110> from 600s to 960s, average grain size decrease considerably until reach the half approximately. After dominant over all texture tilting into <211> from 1080s to 1200s, average grain size increase suddenly and preserve increasing between 99 nm and 106 nm

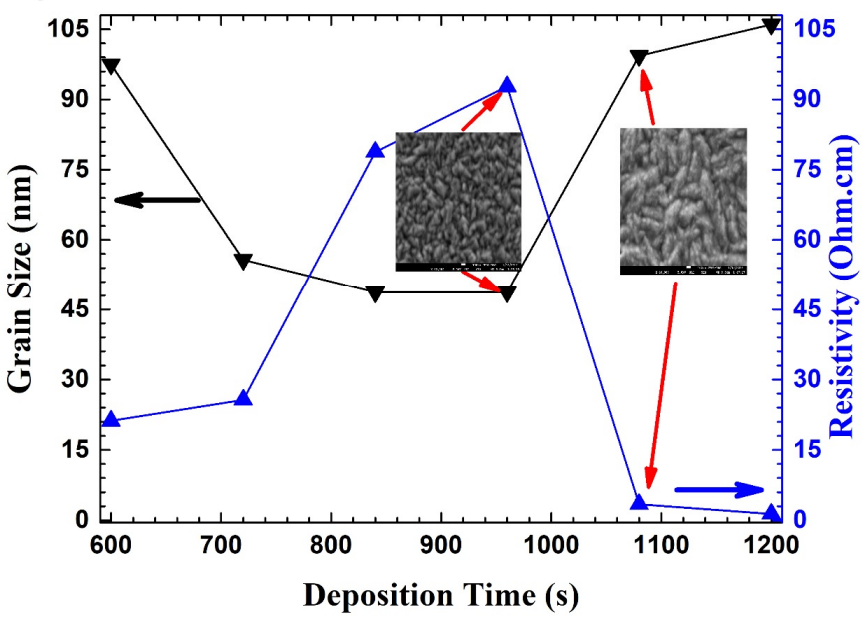

Fig. 5. Dependence of average grain Size and resistivity of $Ni_{1-x}Fe_x$ films on electrodeposition time. SEM images are used as inset to show average grain size change.

respectively (see Table 3). To highlight the granular size change induced by texture tilt <110> into <211> we have join tow SEM images as inset in Fig. 5. We have revealed that dominant texture tilt affect considerably the average grain size and not alloy compositional. This result disagreed with Sam et *al* [30] report. The authors claim that $Ni_{1-x}Fe_x$ with Ni domination (permalloy) compositional affect remarkably the average grain size. Thus, may our result validation is restricted for NiFe alloy with Fe domination.

Resistivity evolution under dominant texture tilt

Using the direct contact of Van Der Paw measurement metallic probes applied on $Ni_{1-x}Fe_x$/ITO/Glass, obtained values of square resistances cannot be attributed to the $Ni_{1-x}Fe_x$ films solely since the commercial ITO covering glass can conduct electricity. For measurement accuracy, the ratio: vertical/horizontal should be respected to be near to the perfect value of 1. To purify $Ni_{1-x}Fe_x$ films we could proceed as follow:

$$R_{sq1} = \frac{R_{sq} \cdot R_{sq2}}{R_{sq2} - R_{sq}} \quad (1)$$

When R_{sq}, R_{sq1} and R_{sq2} are, respectively, the total, $Ni_{1-x}Fe_x$ thin films and ITO films coating glass support square resistances (all in Ω).

The dependence of Resistivity ρ on grains size D under experimental conditions of times deposition of our studied $Ni_{1-x}Fe_x$ alloy films is shown in Fig. 5. It can be seen that the D decrease from 97.5 nm to 48.73 nm while ρ increase from 21, 20 Ω.cm to 92, 78 Ω.cm with increasing time electrodeposition from 600 to 960 s. Resistivity ρ can reaches a minimum value of about 1,35 Ω.cm at 1200 s while D increase, disproportionally, till reach the value of 106.02 *nm*.

Indeed, several phenomena can contribute in thin films electrical resistivity such as: diffusion by the surface, diffusion by the grain boundaries, impurities, defects and magnetic disorder, high preferred orientation. As was suggested by Matthiessen, the resistivity ρ_f can be written as follow:

$$\rho_f = \rho_r + \rho_T \quad (2)$$

Where ρ_T is due to the electron phonon interaction and ρ_r is the residual resistivity which is the sum of the various contributions:

$$\rho_r = \rho_i + \rho_d + \rho_m + \rho_g + \rho_s \quad (3)$$

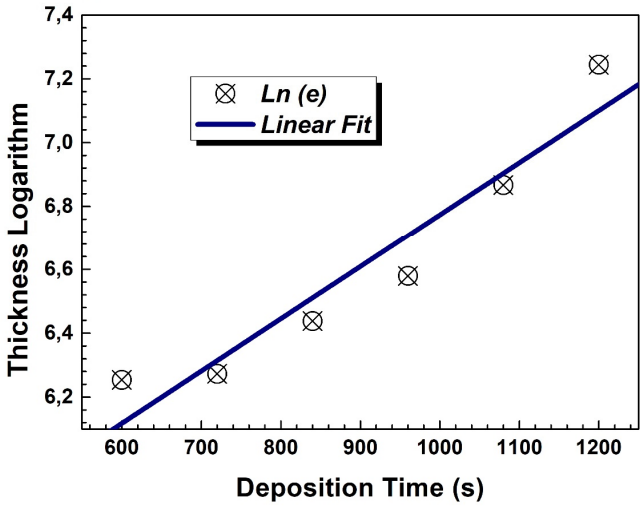

Fig. 6. Films thicknesses-times electrodeposition dependence of $Ni_{1-x}Fe_x$ films. The solid lines are given by the standard logarithmic linear equation; fit parameters are mentioned in subsection 3.3.

Here, ρ_i, ρ_d, ρ_m, ρ_g and ρ_s denote, respectively, the contribution of the impurities, the defects, and the magnetic disorder, the diffusion by the grain boundaries and the diffusion by surface. Besides, we can suggest that eq.(2) can be written separately for each preferred orientation when more than one can be occurring during experience.

In addition, thermal annealing is another important factor that may affect the resistivity of $Ni_{1-x}Fe_x$ alloys. Xiaobai Chen et *al* [29] have found in the case of alloy $Ni_{33}Fe_{67}$ that the values of resistivity was about 8.7 at room temperature and reach 2.7 ($\times 10^{-6}\Omega$m) at 753°K with enhancing vacuum annealing.

It is known that if grain size becomes smaller, grain boundaries number increases. Consequently, diffusion at grain boundaries enhance, thus explains why electrical resistivity has raised in our films. The texture tilt (see Fig.2) beyond 1080 second from <110> into <211> might be another fact directly, assigned to the brutal electrical resistivity fall down. One can say that <211> texture could be characterized by an easier electrical diffusion process at grain boundaries that <110>.

Thickness evolution under dominant texture tilt

In Fig. 6. we present thicknesses variation of our films with respect to times electrodeposition. That increase monotonously between 520 nm and 1400 nm for 600 s and 1200 s respectively (see Table 3). Two stages, before/after texture tilt, can be distinguished for that evolution of thickness. In first stage, when dominant texture was <110> from 600s to 960s, we reveal a thickness gain of 200 nm during 360s electrodeposition time gain. While, for <211> tilted texture, gained thickness in about 440 nm just for only a supplementary 120 s electrodeposition time. At probably, NiFe alloy textured <211> yield more thickness growth than NiFe alloy textured <110>. Mathematically, a slow evolution can be traduced by logarithmic equation. That is why we propose to fit thicknesses versus electrodeposition times to the standard following equation

$$Ln(e) = A \cdot t + B \quad (4)$$

Where *e* and *t* are films thicknesses and times deposition respectively. *A*= 0.001 (in S^{-1}) which have the frequency dimension and *B= 5.135* are the fit constants. Fit was done within minimal (relatively neglegible) errors, which can be quoted (see Fig. 6). Sumalatha Vasam et *al* [31] have reached for NiFe permalloy the thickness of 28 µm using an electrochemical analyzer of CH Instruments (Model: CHI6087E) in Galvanostatic mode. This is twenty time superior than our highest reached thickness of 1.4 µm. May NiFe Permalloy electrodeposition encourage the growth much more than NiFe abnormal alloy.

Surface morphology under texture tilt

Fig. 7 displays Scanning Electron Microscope

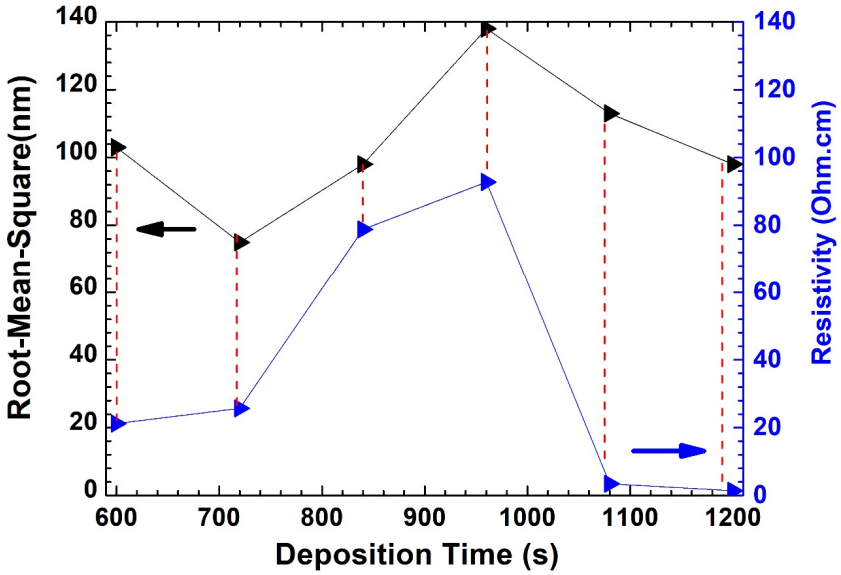

Fig. 7. SEM images of $Ni_{1-x}Fe_x$ (× 40 000) upper films electrodeposited at different times at: a) t=600s, b) t=720s, c) t=840s, d) t=960s,e) t=1080s and f) t=1200s.

SEM images of surfaces morphology of $Ni_{1-x}Fe_x$ films obtained at different electrodeposition times at room temperature. SEM images show clearly a various polycrystalline textures as was suggested by XRD analysis. The surface morphology was found to be greatly influenced by changing time deposition. This is clear to observe by comparing SEM images in figures, which show that all films have grain like structure. It is clearly confirmed, now, that the morphologies of $Ni_{1-x}Fe_x$ films are significantly influenced by dominant texture tilt to <211> (see Fig.7.d and e). As example, at 1080 s, grains size are clearly larger while grain boundaries number is, consequently, decreased. $Ni_{0.14}Fe_{0.86}$, $Ni_{0.19}Fe_{0.81}$ and $Ni_{0.15}Fe_{0.85}$ films have elongated grains Fig.7.d,e and f while all first other $Ni_{0.08}Fe_{0.92}$, $Ni_{0.16}Fe_{0.84}$ and $Ni_{0.15}Fe_{0.85}$ films have rounded grains (Fig.7.a,b and c). Fig.7.a,b shows that in both $Ni_{0.08}Fe_{0.92}$, $Ni_{0.16}Fe_{0.84}$ films, small grains have coalesced to form a smoother film cross section. All films show good adhesion with ITO coated glass substrates.

Discussion of correlations and relationships

In Table 3 we have summarized results of roughness of our $Ni_{1-x}Fe_x$ alloys films that take a change between 75-183 nm. Penny Tsay et *al* [32] have suggested for prepared films using Pulse-reverse electroplating technique, that when Fe becomes the main component, the roughness factor is generally increased and reaches the maximum value in case of pure Fe deposit. M. Saitou et *al* [33] have reported that preferred orientation in NiFe/ITO is strongly influenced by preferred orientation. We have remarked that increase in Fe contents does not meet an agreement with roughness values in our films. In Fig.8, it is clear that for all studied samples, roughness allure correlate well with electrical resistivity, as well with average grain size. This can be explained as follow: when grains become larger, the roughness must be lowered and electrical current density opposing alloy resistivity will traveling less grain boundaries then less obstacles during diffusion. Both of them, electrical resistivity and average grain size obey texture tilt from <110> onto <211>; thus, roughness also is indirectly depend on it. For the best of our knowledge, the roughness depends on the films growth mechanism not the composition of alloy. In similar context, we have remarked that compositional does not influence electrical resistivity and average grain size. Thickness values were depending on texture tilt. Their slow down increase allowed logarithmic fit that was established successfully. In Fig.8, we can confirm the close relationship between of resistivity and roughness. One can see that all details of roughness allure meet those of resistivity. Average grains size, resistivity, thichness and surface roughness was clearly justified by

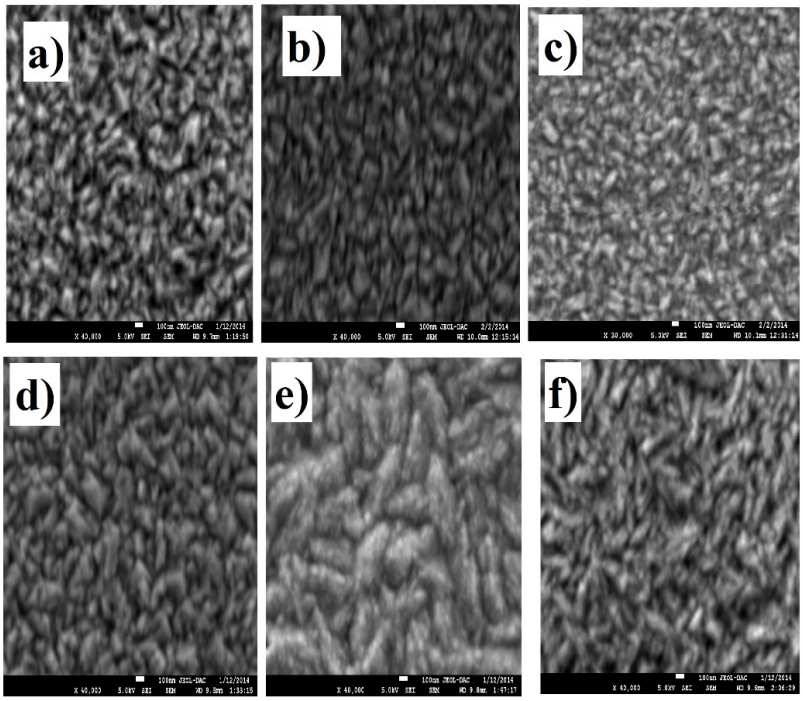

Fig. 8. Surface roughness and Resistivity of $Ni_{1-x}Fe_x$ films dependence on electrodeposition time.

our observed SEM surface micrographs. But NiFe composition seems to be independent in this work that we sincerely think that can be managed by only one fact which, is the abnormal behavior of $Ni_{1-x}Fe_x$ alloy.

CONCLUSIONS

In this work, we have using electrodeposition from a concentrated Fe and Ni sulfamate bath of 0.1 M to electrodeposit Ni_{1-x}Fex/ITO/Glass. Electrodeposition of samples was carrying out using various potentials and times. As changing potential between -1.45 and -1.48 V, we have electrodeposited about four successful samples of Ni_{1-x}Fex/ITO/Glass. Their investigation can be qualified as a routine study, that we have not focus a lot on them. Although we have used an unusual potential range between -1.45 V and -1.48 V. Whereas, changing electrodeposition time seems to be very important since we reveal an overall texture tilt from <110> onto <211>. Hence, microstructure, morphology, electrical resistivity, thickness and roughness are all remarkably affected. Our main results about the influence of texture change on the $Ni_{1-x}Fe_x$/ITO/Glass, structural, electrical and morphological properties are also summarized. Thus, the X-ray patterns studies of electrodeposited Ni_{1-x}Fex/ITO/Glass for various potentials and times at room temperature revealed the existence of bcc phase as the dominant structure. Enhancing electrodeposition potential did not affect $Ni_{1-x}Fe_x$ global textures or the dominant one except some curvatures that may affect surface smooth of final samples. Whereas, enhancing electrodeposition time shows texture tilt from (110) to (211) revealed for first time at 1080s. This can make part of the general behaviour of $Ni_{1-x}Fe_x$ abnormal alloy. After texture tilt, the rest of study was built on their influence that we have distinguished the cases before/after texture tilt. NiFe alloy textured <211> yield thicker NiFe films (960 to1400 nm) than the one textured <110> and average grain size become almost larger reached 99 to 106 nm. Diffusion at the grain boundaries seems to be the predominant factor controlling electrical resistivity and not directly the grain size. Lowest Resistivity ρ of about 1,35 Ω.cm at 1200 s was reached with tilted texture <211> making NiFe <211> more conductor that NiFe <110>. Indeed overall texture tilt have made NiFe alloy more performant and more interesting. Fe content (%wt) in electrodeposited $Ni_{1-x}Fe_x$ films compositional have changed between about 82-92%. Average grain size, electrical resistivity,

thickness and roughness seem to not correlate with electrodeposited $Ni_{1-x}Fe_x$ films compositional. We prove that resistivity, grain size and roughness are highly correlated between each other's and some relationships was presented and judged within available SEM images.

Our main perspective after carrying out the present work is to going through electrodeposition of Invar $Fe_{64}Ni_{36}$ with <200> overall texture using the same sulphate bath. This will be possible with optimizing and mastery some electrochemical parameters (such as precursor PH and concentration), since we have remarked co-existence of Invar alloy presented by <200> texture in films electrodeposited at 600 s wherever the used potential (see Fig.2.b).

ACKNOWLEDGMENTS

We would like to acknowledge La Direction Générale de la Recherche Scientifique et du Développement Technologique (DGRSDT), Algeria. Moreover, we send sincere thanks to Laboratory for Developing New Materials and their Characterizations, University of Setif1, Algeria.

CONFLICT OF INTEREST

The authors declare that there is no conflict of interests regarding the publication of this manuscript.

REFERENCES

1. Aravinda CL, Mayanna SM. Potentiostatic Deposition of Thin Films of Ni-Fe Alloys. Transactions of the IMF. 1999;77(2):87-88.
2. Li H, Ebrahimi F. Synthesis and characterization of electrodeposited nanocrystalline nickel–iron alloys. Materials Science and Engineering: A. 2003;347(1-2):93-101.
3. Morioka S, Takahashi M, Sawada Y, Shimodaira S, Ogawa S. The Preparation of 80%Ni-Permalloy Films by Electrodeposition and Their Magnetic Properties. Journal of the Japan Institute of Metals. 1961;25(10):679-683.
4. Thompson BJ, Wolf E. Two-Beam Interference with Partially Coherent Light. Journal of the Optical Society of America. 1957;47(10):895.
5. Wolf J. W., Proc. Am. Electroplaters'Soc. 1956, 43: 215.
6. Wolf J. W. and Katz H. W., Proc. Electronic Component Conf., Philadelphia, PA, 1959, pp. 15 - 20.
7. Bozorth RM. The Orientations of Crystals in Electrodeposited Metals. Physical Review. 1925;26(3):390-400.
8. Sallo JS, Carr JM. Magnetic Electrodeposits of Cobalt-Phosphorus. Journal of The Electrochemical Society. 1962;109(11):1040.
9. Smith RS, Godycki LE, Lloyd JC. Effects of Saccharin on the Structural and Magnetic Properties of Iron-Nickel Films. Journal of The Electrochemical Society. 1961;108(10):996.
10. Kirkpatrick BM, Masse J. GALVANOMETERS, PROJECT VT/072. Defense Technical Information Center; 1964 1964/12/17.
11. Lainer DI, Ostrovskaya LM, Épshtein MG, Kochkarev VI, Khavricheva VP. Method of Preparing Stable n-Type Material for Thermoelements Working under Cooling Conditions. Thermoelectric Properties of Semiconductors: Springer US; 1964. p. 89-93.
12. Shreir LL. Appendix — The Potential Difference at a Metal/Solution Interface. Corrosion: Elsevier; 1976. p. 9:71-79:87.
13. Wiess RJ. Proc Phys Soc, 1963:; 82:281.
14. The magnetization of face-centred cubic and body-centred cubic iron + nickel alloys. Proceedings of the Royal Society of London Series A Mathematical and Physical Sciences. 1963;272(1348):119-132.
15. Kouvel JS, Wilson RH. Magnetization of Iron-Nickel Alloys Under Hydrostatic Pressure. Journal of Applied Physics. 1961;32(3):435-441.
16. A. Brenner: Electrodeposition of Alloys. Principle and Practice. Academic Press, New York and London 1963. Band I: General Survey, Principles, and Alloys of Copper and of Silver. 714 S. mit 212 Bildern und 45 Tab. DIN A5. Preis: $ 24. Berichte der Bunsengesellschaft für physikalische Chemie. 1964;68(3):309-309.
17. Dahms H, Croll IM. The Anomalous Codeposition of Iron-Nickel Alloys. Journal of The Electrochemical Society. 1965;112(8):771.
18. Krause T, Arulnayagam L, Pritzker M. Model for Nickel-Iron Alloy Electrodeposition on a Rotating Disk Electrode. Journal of The Electrochemical Society. 1997;144(3):960-969.
19. Qi B, Ni X, Li D, Zheng H. A Facile Non-hydrothermal Fabrication of Uniform α-MoO3Nanowires in High Yield. Chemistry Letters. 2008;37(3):336-337.
20. Su C-w, He F-j, Ju H, Zhang Y-b, Wang E-l. Electrodeposition of Ni, Fe and Ni–Fe alloys on a 316 stainless steel surface in a fluorborate bath. Electrochimica Acta. 2009;54(26):6257-6263.
21. Tabakovic I, Inturi V, Thurn J, Kief M. Properties of Ni1–xFex (0.1<x<0.9) and Invar (x=0.64) alloys obtained by electrodeposition. Electrochimica Acta. 2010;55(22):6749-6754.
22. Liu B, Huang R, Wang J, Widatallah HM, Lu H, Zhang J, et al. Mössbauer investigation of Fe–Ni fine particles. Journal of Applied Physics. 1999;85(2):1010-1013.
23. Djekoun A, Boudinar N, Chebli A, Otmani A, Benabdeslem M, Bouzabata B, et al. Structure and magnetic properties of Fe-rich nanostructured Fe100−XNiX powders obtained by mechanical alloying. Physics Procedia. 2009;2(3):693-700.
24. Ghebouli B, Chérif SM, Layadi A, Helifa B, Boudissa M. Structural and magnetic properties of evaporated Fe thin films on Si(111), Si(100) and glass substrates. Journal of Magnetism and Magnetic Materials. 2007;312(1):194-199.
26. Chen X, Qiu H, Wu P, Wang F, Pan L, Tian Y. Phase transformation of Ni33Fe67 and Ni21Fe79 films grown on SiO2/Si(100). Physica B: Condensed Matter. 2005;362(1-4):255-265.
26. Oleszak D, Shingu PH. Mechanical alloying in the Fe?Al system. Materials Science and Engineering: A. 1994;181-

182:1217-1221.
27. Hamzaoui R, Elkedim O, Fenineche N, Gaffet E, Craven J. Structure and magnetic properties of nanocrystalline mechanically alloyed Fe–10% Ni and Fe–20% Ni. Materials Science and Engineering: A. 2003;360(1-2):299-305.
28. Sam S, Fortas G, Guittoum A, Gabouze N, Djebbar S. Electrodeposition of NiFe films on Si(100) substrate. Surface Science. 2007;601(18):4270-4273.
29. Cheung C, Nolan P, Erb U. Synthesis of nanocrystalline permalloy. Materials Letters. 1994;20(3-4):135-138.
30. Buchheit TE, Goods SH, Kotula PG, Hlava PF. Electrodeposited 80Ni–20Fe (Permalloy) as a structural material for high aspect ratio microfabrication. Materials Science and Engineering: A. 2006;432(1-2):149-157.
31. Vasam S, Srinivas V. Microstructure and magnetoimpedance studies of NiFe films electrodeposited on ITO substrate: Experiments and simulations. Journal of Magnetism and Magnetic Materials. 2020;514:167154.
32. Min L, Kuo-Chin L, Chi-Chang S, Yu-Tsung W, Chun-Sheng F, Yu-Cheng L. An electroporation microchip for gene transfection and system optimization. IEEE International Conference on Mechatronics, 2005 ICM '05: IEEE.
33. Saitou M, Oshikawa W, Mori M, Makabe A. Surface Roughening in the Growth of Direct Current or Pulse Current Electrodeposited Nickel Thin Films. Journal of The Electrochemical Society. 2001;148(12):C780.